A Diagnostic Study of Eddy–Mean Flow Interactions during FGGE SOP-1

MARK P. BALDWIN, H. J. EDMON, JR. AND JAMES R. HOLTON

Department of Atmospheric Sciences, University of Washington, Seattle, Washington 98195

(Manuscript received 2 November 1984, in final form 18 April 1985)

ABSTRACT

Eliassen–Palm (EP) diagrams have been shown to be very useful diagnostics in both the troposphere and the stratosphere. However, the idea that the EP flux divergence is the sole forcing of the mean wind by the eddies can be misleading. A time series of the time rate of change of the zonal mean wind and the EP flux divergence shows that the two quantities were not well correlated during the FGGE special observing period (SOP-1, winter 1979). Calculation of the residual in the zonal momentum equation reveals that considerable negative acceleration (drag) is required to complete the momentum balance in some regions. This residual indicates that not all terms are well represented in atmospheric data sets, and may be largely due to the breaking of vertically propagating gravity waves near the tropopause.

Eliassen–Palm diagrams are presented for the FGGE data, as well as Oort's 11-year climatology. The Oort EP diagrams serve as a standard with which to compare other EP diagrams. The FGGE year is shown to be very similar to climatology. A consistent method of displaying the EP flux vectors and divergence is suggested, which has advantages over previous methods.

1. Introduction

The feedback of zonally asymmetric eddies on the zonal mean flow is one of the basic processes determining the nature of the general circulation. It is well known that the existence of large-amplitude eddy heat and momentum fluxes does not necessarily imply that there is significant mean flow driving by eddies since such fluxes can be compensated for by an eddy-driven ageostrophic circulation.

Andrews and McIntyre (1976) and Boyd (1976) showed that the net eddy forcing can be efficiently represented by the divergence of a vector in the meridional plane that is now called the "Eliassen–Palm" (EP) flux. Edmon *et al.* (1980) showed that latitude–height cross sections of the EP flux provide very useful diagnostics for understanding the interaction between zonally asymmetric disturbances and the zonal mean circulation. They found, for example, that EP flux divergence patterns for numerical simulations of nonlinear baroclinic waves closely resembled midlatitude tropospheric patterns computed from two independent data sets.

More recently, Dunkerton *et al.* (1981), Palmer (1981) and others have found that the EP flux is a useful diagnostic for wave driving of the mean flow in stratospheric sudden warmings. Hartmann *et al.* (1984) produced correlations between the time rate of change of the mean zonal wind and the EP flux divergence for the Southern Hemisphere and found that the two quantities are closely related near the tropopause and in the middle to upper stratosphere.

Although the EP flux vector provides a useful measure of quasi-geostrophic wave propagation in the troposphere, it is not clear whether its divergence is closely correlated with the zonal flow deceleration, as in the case of the stratosphere during warmings. It is shown in this paper that during FGGE SOP-1 (first special observing period) these quantities were not closely related and that the computed zonal momentum balance had a substantial residual. This residual can be interpreted as evidence for zonal mean drag by unresolved scales of motion—possibly gravity waves breaking near the tropopause.

2. Basic equations and theoretical background

Most of the relevant theory is given in Edmon *et al.* (1980) and Palmer (1981). In log-pressure coordinates, the zonal mean equations in quasi-geostrophic scaling are

$$\frac{\partial \bar{u}}{\partial t} = f\bar{v} - \frac{1}{r_0 \cos^2\phi}\frac{\partial}{\partial \phi}(\cos^2\phi \overline{u'v'}) + \bar{G} \qquad (1)$$

$$\frac{\partial \bar{\theta}}{\partial t} = -\bar{\theta}_z \bar{w} - \frac{1}{r_0 \cos\phi}\frac{\partial}{\partial \phi}(\cos\phi \overline{v'\theta'}) + \bar{Q} \qquad (2)$$

where

$$z = -H\ln(P/1000 \text{ mb}) \qquad (3)$$

and $\bar{G}$ denotes the force due to unresolved eddies. Other notation follows Palmer (1981). If we define a "residual" mean meridional circulation ($\bar{v}^*$, $\bar{w}^*$) by letting

$$\bar{v}^* \equiv \bar{v} - \exp(z/H)\frac{\partial}{\partial z}\left[\exp(-z/H)\frac{\overline{v'\theta'}}{\bar{\theta}_z}\right] \qquad (4)$$

$$\bar{w}^* \equiv \bar{w} + \frac{1}{r_0 \cos}\frac{\partial}{\partial\phi}\left[\cos\phi\,\frac{\overline{v'\theta'}}{\bar{\theta}_z}\right], \tag{5}$$

the zonal mean equations may then be written in the transformed Eulerian mean form as:

$$\frac{\partial\bar{u}}{\partial t} - f\bar{v}^* - \bar{G} = \frac{\nabla\cdot\mathbf{F}}{r_0\cos\phi\,\exp(-z/H)} \tag{6}$$

$$\frac{\partial\bar{\theta}}{\partial t} + \bar{\theta}_z\bar{w}^* - \bar{Q} = 0 \tag{7}$$

with

$$\mathbf{F} = r_0\cos\phi e^{-z/H}[-\overline{u'v'}, f\overline{v'\theta'}/\bar{\theta}_z]. \tag{8}$$

Thus, divergence of the EP flux [scaled by $(r_0\cos\phi)^{-1}\exp(z/H)$] is the sole forcing of the mean flow by meteorological eddies. According to the "nonacceleration theorem" (Charney and Drazin, 1961), for steady conservative waves $\nabla\cdot\mathbf{F} = 0$, and there is no net forcing of the mean flow by the waves. If $\bar{Q}$ and $\bar{G}$ also vanish, then a steady mean flow exists.

Divergence of the EP flux also gives the northward transport of quasi-geostrophic potential vorticity. Palmer (1982) has shown that in spherical coordinates this relationship has the form:

$$\overline{v'q'}_{(m)} = \nabla\cdot\mathbf{F}(r_0\cos\phi e^{-z/H}) \tag{9}$$

where $q'_{(m)}$ is a modified eddy quasi-geostrophic potential vorticity given by

$$q'_{(m)} = v'_x - \frac{f}{\cos\phi}\left[\frac{\cos\phi}{f}u'\right]_y + f\left[\frac{\theta'}{\bar{\theta}_z}e^{-z/H}\right]_z e^{z/H}. \tag{10}$$

The EP flux is also important in wave theory. A conservation relation of the form

$$\frac{\partial A}{\partial t} + \nabla\cdot\mathbf{F}(r_0\cos\phi e^{-z/H}) = D \tag{11}$$

was derived by Andrews and McIntyre (1976, 1978). See Strauss (1983) for a review of the subject. For conservative motion D is zero and A can be called the EP wave activity

$$A \approx \frac{1}{2}\left(\frac{\overline{q'^2}}{\bar{q}_y}\right).$$

For planetary scale waves for which WKBJ theory holds,

$$\mathbf{F} = \mathbf{C}_g A$$

where $\mathbf{C}_g$ is the group velocity of the waves. Thus, within these approximations, wave energy will propagate parallel to $\mathbf{F}$.

3. The data sets and plotting conventions

The data set consists of the FGGE analysis for SOP-1, 5 January to 3 March 1979 from Goddard Space Flight Center analyses (experiments number 2254, 2274 and 2282); U, V, T, Φ and ω were available at 0000 GMT and 1200 GMT daily on a 4° latitude by 5° longitude grid (46 × 72) that covered the entire globe. The data were available at the twelve standard pressure levels from 1000 to 50 mb (1000, 850, 700, 500, 400, 300, 250, 200, 150, 100, 70, 50 mb). Only the Northern Hemisphere data were used for the calculations.

It is expected that the FGGE SOP-1 data set, because of the large number of observations available, should provide an excellent representation of the atmosphere during that period.

The Oort (1983) climatology will be used to compare with the FGGE data set. The Oort statistics were derived from eleven years of station data (1963–1973) and covered both hemispheres from 80°S to 80°N. The three month winter period (December, January and February) will be used as a comparison.

The Oort statistics are probably the best representation of the zonal mean climatology available. A comparison between the FGGE data and the Oort statistics should reveal how FGGE SOP-1 differed from the climatological average winter. It is also possible that the high quality of the FGGE data will allow some features to be discerned that were not captured in the Oort analyses.

A major objective of the present paper is to compare EP flux cross sections for these two data sets.

A single convention for plotting the EP cross sections has not yet emerged. The EP diagrams shown here differ somewhat from those in Edmon *et al.* The diagrams shown here use log p as a vertical coordinate, whereas Edmon *et al.* used p as a vertical coordinate and plotted a modified EP flux divergence [see their Eqs. (3.10) to (3.13)]. The quantity plotted here is

$$\nabla\cdot\mathbf{F}/(r_0\cos\phi e^{-z/H})$$

which clearly shows the net driving force by the eddies on the mean flow with contours in m s^{-1} (day)$^{-1}$.

Edmon *et al.* have plotted cross sections of $\mathbf{F}(y, p)$ scaled so that the arrows appear nondivergent if and only if $\nabla\cdot\mathbf{F} = 0$. This scaling inevitably emphasizes the lower troposphere due to the factor $\exp(-z/H)$ in $\mathbf{F}$. Also, for $\mathbf{F}$ to appear nondivergent when $\nabla\cdot\mathbf{F} = 0$, $\mathbf{F}$ must be multiplied by a factor proportional to $\cos\phi$ (Palmer, 1981).

However, if one is willing to obtain the divergence of $\mathbf{F}$ only from the contours of $\nabla\cdot\mathbf{F}$, then $\mathbf{F}$ can be scaled by $\exp(z/H)$ [canceling $\exp(-z/H)$] and the $\cos\phi$ factor can be omitted. This has the principle advantage that a vector of a given length will always represent the same magnitudes of $-r_0\cos\phi\overline{u'v'}$ and $r_0 f\cos\phi\overline{v'\theta'}/\bar{\theta}_z$ [see Eq. (8)]. Thus, more information about the individual heat and momentum fluxes can be obtained from the diagram, and the orientation of the arrows is preserved. Also, the arrows no longer become very small at high altitudes because the $\exp(-z/H)$ factor has been removed.

In practice, the fact that such arrows appear slightly divergent when $\nabla \cdot \mathbf{F} = 0$ is not a problem since the effect is small and difficult to see, and the divergence is immediately determined by the contours of $\nabla \cdot \mathbf{F}$. This convention for displaying both the vectors and the flux divergence is more practical than other conventions for studies of eddy–mean flow interaction.

4. Results

a. Zonal mean wind, momentum fluxes and heat fluxes

Before presenting the EP diagrams for the FGGE data and the Oort climatology, it is helpful to examine the zonal mean wind and eddy flux cross sections for the FGGE data. References will be made to the corresponding figures in Oort (1983). For the FGGE data set, transient eddies are defined as deviations from a 58 day average, while a 90 day average is used in the Oort data set. This difference can be expected to account for some of the differences between the FGGE data set and Oort's climatology.

Since the FGGE data set covers only one winter, one cannot expect that it should agree closely with a long-term climatology.

The zonal mean wind component (Fig. 1) is very similar to that of the climatological distribution (Oort's Fig. A41) in the middle and high latitudes. Both the location and strength of the jet match well with climatology. However, the lack of easterlies between 200 and 500 mb in the tropics is atypical. The FGGE SOP-1 zonal mean wind differed significantly from climatology in the tropical troposphere.

The northward transport of momentum by the transient eddies (Fig. 2) is very similar to that in Oort's climatology (Oort's Fig. A49). The corresponding transport of momentum by the stationary waves (Fig. 3) is less representative of the climatological values.

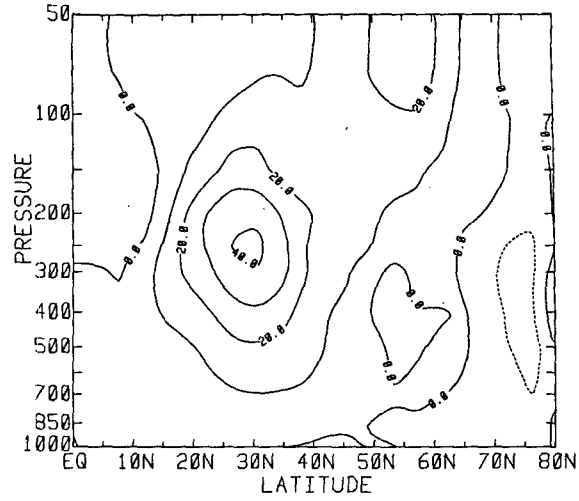

FIG. 2. Zonal mean northward momentum transport by transient eddies for FGGE SOP-1 data. Contour interval of 10 $m^2 s^{-2}$.

The maximum northward transport is somewhat weaker, but is located in the same region as the climatological maximum, at about 30°N and 200 mb. Farther to the north, the equatorward transport is much stronger than the climatological values, and its maximum is found at a somewhat lower level.

Figure 4 shows the northward transport of heat by the transient eddies. There are two features that differ significantly from climatology (Oort's Fig. A50). The most obvious is a maximum at about 10°N and 200 mb. This feature, which is absent in the Oort statistics, contributes to a substantial vertical component of the EP flux (especially considering the low static stability in the region).

The maximum above 100 mb north of 50°N is unusually large, reflecting the very active stratosphere

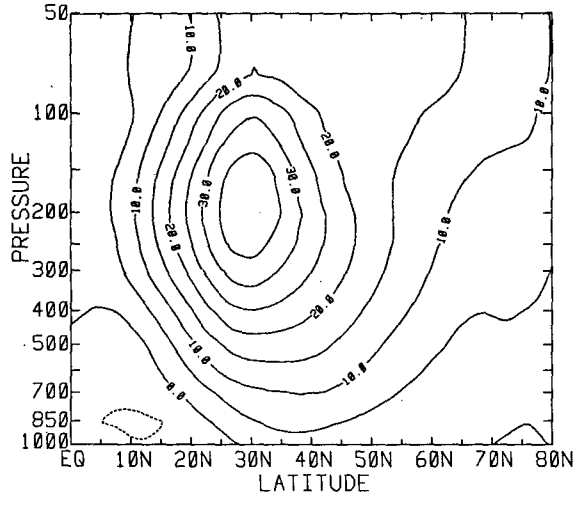

FIG. 1. Zonal mean wind distribution for FGGE SOP-1 data. Contour interval of 5 m s^{-1}.

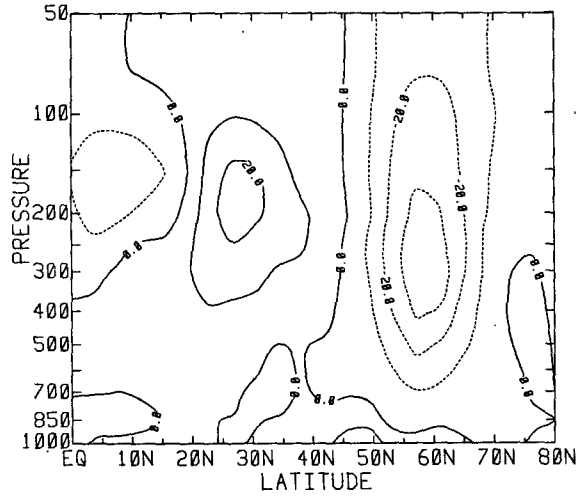

FIG. 3. As in Fig. 2 but by stationary waves.

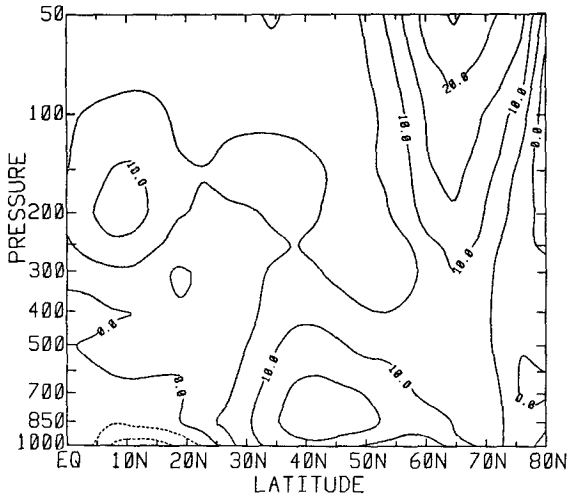

FIG. 4. Zonal mean northward heat transport by transient eddies for FGGE SOP-1 data. Contour interval of 5 m s^{-1} K.

during January–February 1979. The rest of the region is in good agreement with the Oort climatology.

Figure 5 shows the corresponding heat transport by the stationary waves. The agreement with climatology is closer. The maximum between 40°N and 70°N is somewhat stronger than the climatological value above 100 mb and weaker below 100 mb, but in general agreement is close.

Overall, the zonal means of the FGGE data set are close to the climatological mean state. There are a few interesting and unusual features, but the agreement with climatology is close enough that results for the FGGE SOP-1 are likely to be fairly typical.

b. *Eliassen–Palm diagrams*

The EP diagrams, Figs. 6a–6f, show transient, stationary, and total wave EP fluxes for both the FGGE and Oort data sets. In general, the FGGE diagrams are quite similar to those for the Oort climatology, but with a few interesting differences.

We will first compare the Oort EP diagrams with corresponding figures in Edmon *et al.* (Figs. 1b, 4b and 5b) which were produced from Oort and Rasmusson's (1971) 1958–63 data set. The Oort EP diagrams shown in this paper were produced from Oort's 1963–73 data set. As with the basic fields, the transient waves are defined as deviations from the time averages of 58 days for the FGGE data and 90 days for the Oort statistics. Thus, the partitioning between the transient and stationary components is slightly different. By this definition, transient eddies include variations on time scales of more than one month.

A comparison of the Oort EP diagrams with the corresponding diagrams is Edmon *et al.* shows that there were differences in the data sets as well as the resolution below 850 mb. The general pattern of the EP flux is very similar, but the Oort data set shows more pronounced divergence in the lower stratosphere. The Oort diagrams were computed using the 1000, 850 and 700 mb levels (to be consistent with the FGGE diagrams), while the diagrams in Edmon *et al.* include 1000, 950, 900, 850, 700 mb. The lower resolution in the Oort diagrams largely explains the lack of EP flux convergence below 850 mb at about 35°N.

A comparison of Figs. 6a and 6b shows that the pattern of the EP flux arrows is similar, with the exception of the tropics. The stratosphere was definitely more active during the FGGE winter, and there is some disagreement in the high latitude and midtroposphere.

The stationary wave patterns, Figs. 6c and 6d, also look similar, with the stratosphere again being more active during the FGGE period. There is some disagreement in the high latitude midtroposphere, but the disagreement is in the opposite sense from that in the transient eddy diagrams.

The high latitude differences may be largely due to the partitioning between transient and stationary waves. As can be seen in Figs. 6e and 6f, the effects nearly cancel when the transient and stationary components are summed, resulting in remarkably similar EP diagrams.

The two main unusual features of the FGGE SOP-1 EP diagrams are the strong divergence in the lower stratosphere and the large upward EP flux in the tropics.

c. *Five-day means*

The FGGE data set includes the period of the major stratospheric sudden warming in late February (Quiroz, 1979; Palmer, 1981). In order to examine changes in wave propagation and eddy–mean flow interaction five-day averages of the transient wave EP flux were computed for the entire period. Figures 7a–7d illustrate the changes that took place from 9 February to 28 February 1979, a period that includes the major wavenumber 2 warming.

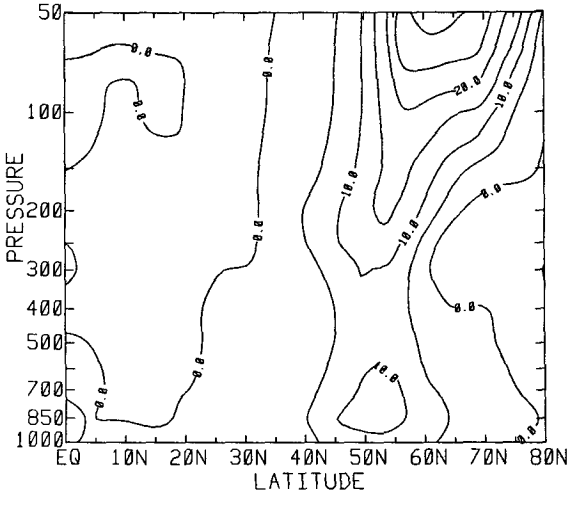

FIG. 5. As in Fig. 4 but by stationary waves.

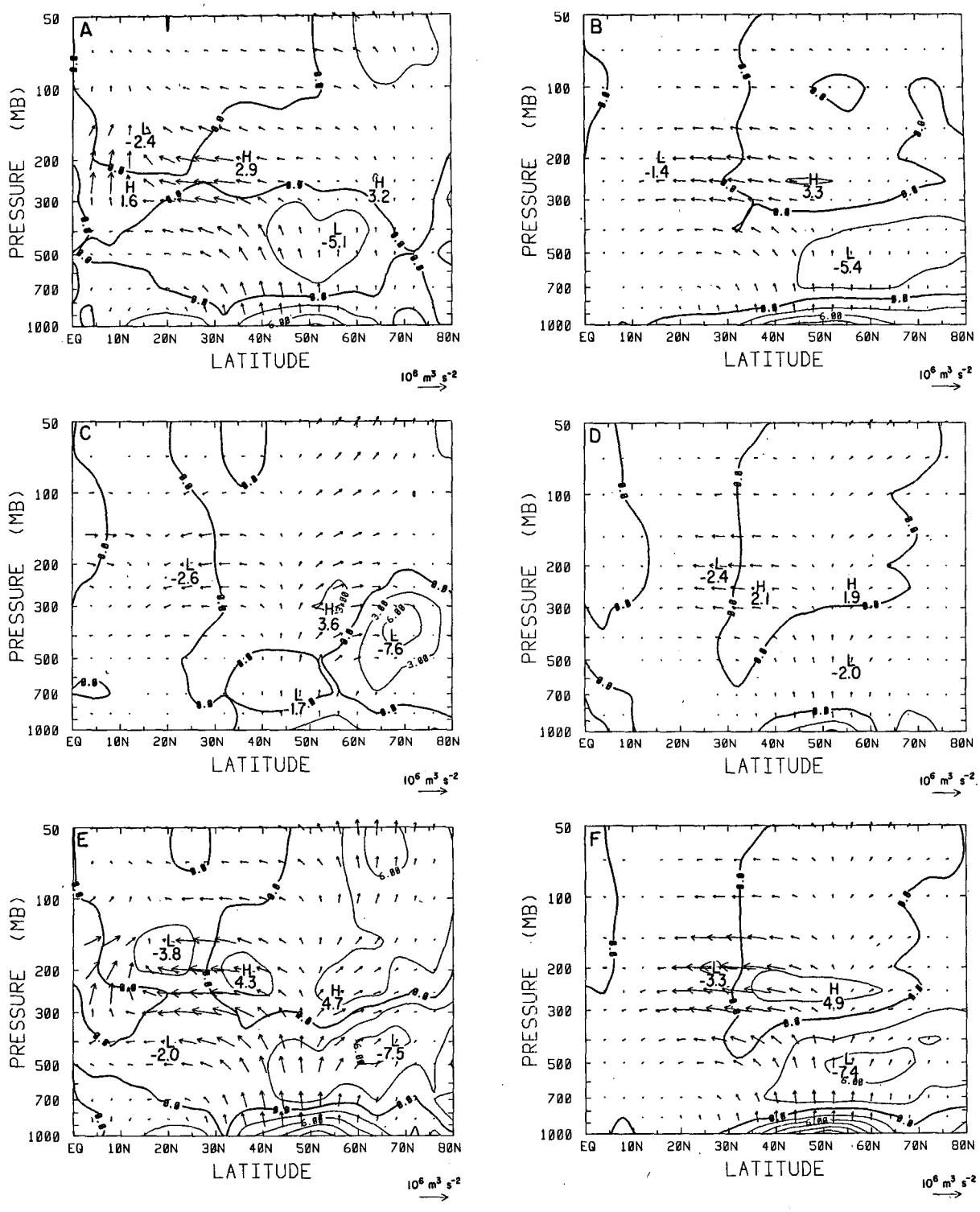

FIG. 6. Eliassen–Palm diagrams for FGGE 58-day mean and Oort 90-day mean winter data. EP flux divergence contour interval of 3 m s^{-1} $(day)^{-1}$. See text for scaling of arrows. (a) FGGE data, transient eddies, (b) Oort data, transient eddies, (c) FGGE data, stationary waves, (d) Oort data, stationary waves, (e) FGGE data, total waves, (f) Oort data, total waves.

The five-day mean patterns are quite noisy, but large changes are easily visible. Figure 7a (9–13 February) does not look too different from the 58 day average. The next period, from 14–18 February, was much more chaotic, with upward and southward wave propagation being less clear. By 19–23 February, the usual north-

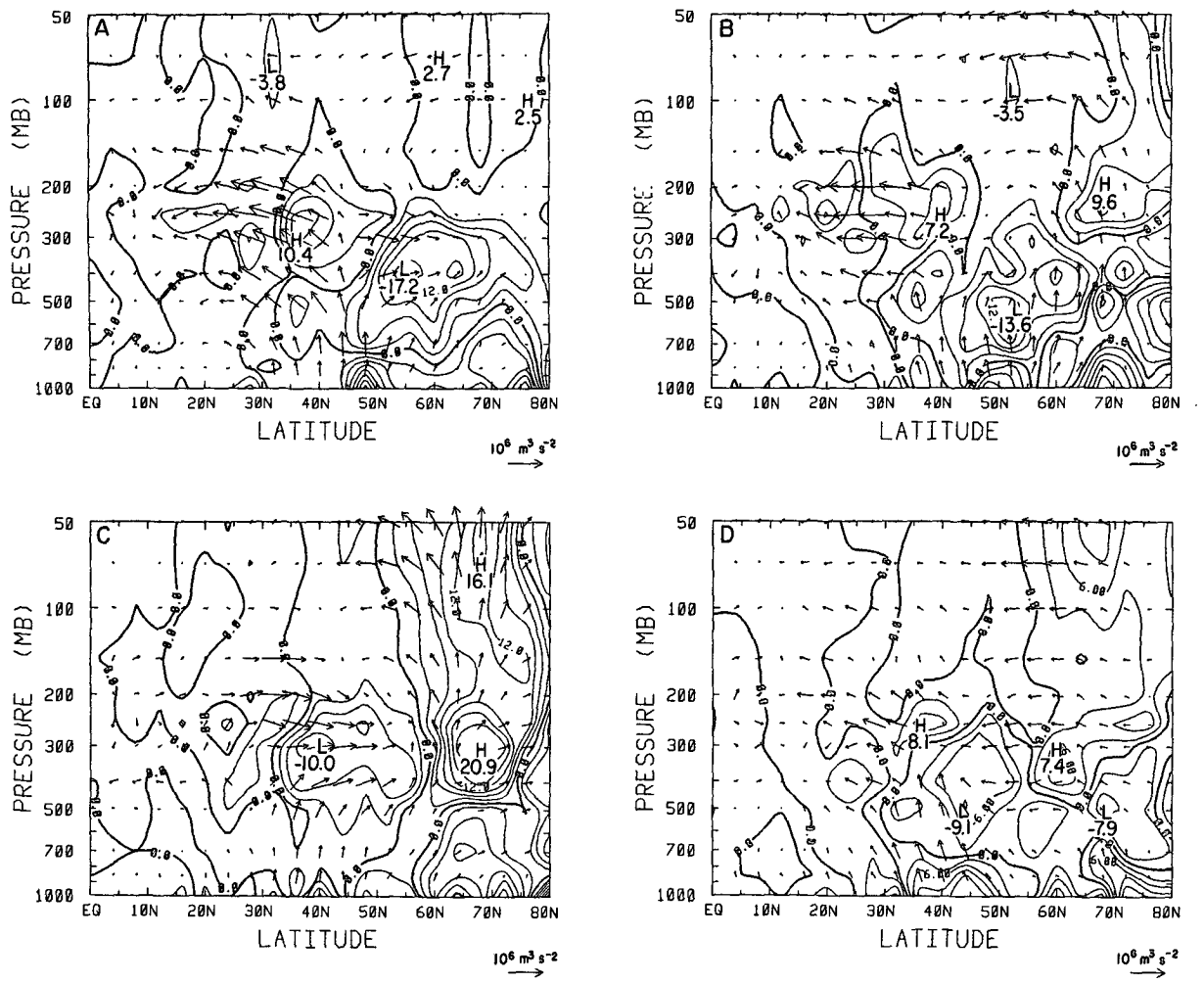

FIG. 7. Five-day mean transient eddy EP flux diagrams for FGGE data. Contour interval of 3 m s^{-1} (day)$^{-1}$. See text for scaling of arrows. (a) 9–13 February, (b) 14–18 February, (c) 19–23 February, (d) 24–28 February.

ward momentum transport had reversed, and massive divergence and upward propagation had developed north of 60°N above 500 mb. The net force on the zonal mean wind exceeded 20 m s^{-1} (day)$^{-1}$. Just as suddenly as it developed, this active region decayed by 24–28 February, with the large source of wave activity seeming to recede into the stratosphere.

It seems unusual that the lower stratosphere had a positive EP flux divergence, indicating an accelerating force on the mean flow during the warming event. A comparison with Palmer's (1981) Fig. 3 shows that Palmer's (Meteorological Office) analysis differs considerably from the FGGE analysis. Although the Meteorological Office analysis shows a divergence of the EP flux after 22 February, it does not show the high latitude divergence which was already present in the FGGE analysis by 14–18 February. During the warming, the zonal wind, at high latitudes above 100 mb, slowed by about 10 m s^{-1}.

d. Time series

Figure 8 shows a daily time series of $\partial\bar{u}/\partial t$ versus $\nabla\cdot\mathbf{F}$ for the FGGE period averaged over the region 36°N to 60°N and 200 mb to 500 mb. This region was picked to represent the midlatitude upper troposphere. Other regions were tried with similar results. The relationship between the two quantities was not strong, with a correlation coefficient of 0.339. The magnitude of the wave driving was typically much greater than $\partial\bar{u}/\partial t$.

For this region, the EP flux divergence was not a good indicator of the zonal mean acceleration. Since the $f\bar{v}^*$ term is significant, the same calculation was done for $\partial\bar{u}/\partial t$ versus $\nabla\cdot\mathbf{F} + f\bar{v}^*$; $\bar{v}$ was calculated directly from the gridded data. This is shown as Fig. 9. The average difference between the variables is less, but the correlation coefficient is only 0.056.

Calculations by Hartmann *et al.* (1984) indicate a

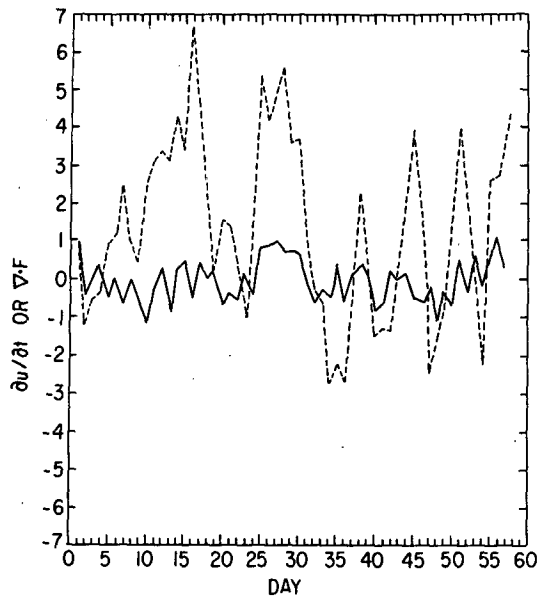

FIG. 8. Time series of $\partial\bar{u}/\partial t$ vs. wave driving for FGGE data, averaged over 36°N to 60°N, 200–500 mb. Solid line represents $\partial\bar{u}/\partial t$. Dashed line represents $\nabla \cdot \mathbf{F}$.

somewhat better relationship between $\partial\bar{u}/\partial t$ and $\nabla \cdot \mathbf{F}$ in the Southern Hemisphere middle stratosphere and near the tropopause. They found correlation coefficients for individual gridpoints in the meridional plane of more than 0.6, with lower correlations in the troposphere.

Clearly, the day-to-day balance is not between $\partial\bar{u}/\partial t$ and $\nabla \cdot \mathbf{F}$. The residual circulation plays an important role. The ageostrophic terms may also be important, as well as wave drag from unresolved eddies.

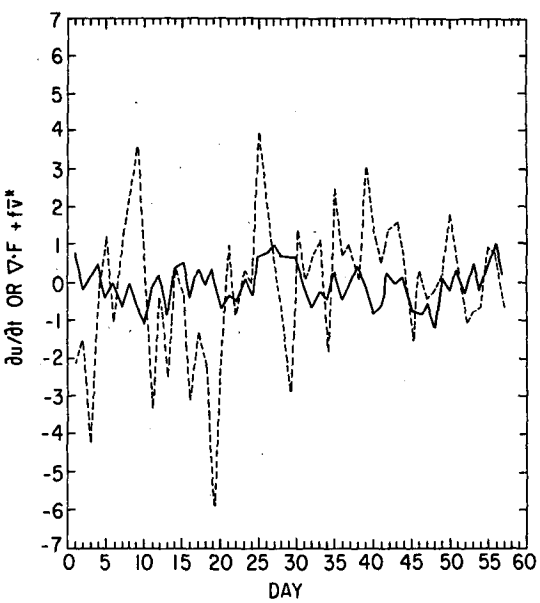

FIG. 9. Time series of $\partial\bar{u}/\partial t$ vs. $\nabla \cdot \mathbf{F} + f\bar{v}^*$ for FGGE data, averaged over 36°N to 60°N, 200–500 mb. Solid line represents $\partial\bar{u}/\partial t$. Dashed line represents $\nabla \cdot \mathbf{F} + f\bar{v}^*$.

e. *The momentum balance*

To further investigate the lack of correlation between $\partial\bar{u}/\partial t$ and $\nabla \cdot \mathbf{F}$, all terms in the full ageostrophic zonal momentum equation [Eq. (12)] were computed for the 58-day average, and the residual was computed.

$$\bar{u}_t = -\bar{v}[(a\cos\phi)^{-1}(\bar{u}\cos\phi)_\phi - f] + \bar{w}^*\bar{u}_z + (\rho_0 a\cos\phi)^{-1}\nabla \cdot \mathbf{F}$$

where

$$\nabla \cdot F \equiv (a\cos\phi)^{-1}\frac{\partial}{\partial\phi}(F^{(\phi)}\cos\phi) + \frac{\partial F^{(z)}}{\partial z} \quad (12)$$

and

$$F^{(\phi)} \equiv \rho_0 a\cos\phi[\bar{u}_z\overline{v'\theta'}/\bar{\theta}_z - \overline{v'u'}]$$

$$F^{(z)} \equiv \rho_0 a\cos\phi[\{f - (a\cos\phi)^{-1} \times (\bar{u}\cos\phi)_\phi\}\overline{v'\theta'}/\bar{\theta}_z - \overline{w'u'}].$$

The residual represents the net unbalanced force which is not balanced by a change in the mean wind. Defined in this way, a region in which the residual is negative indicates that a negative acceleration (or drag) is needed to complete the balance. The result is shown as Fig. 10.

The region north of 72°N did not appear to be reliable and was omitted. In the midlatitudes, especially in the lower stratosphere, considerable negative acceleration would be required to complete the balance. Near 55°N a positive acceleration would be required. A pattern similar to this has been computed by T. N. Palmer (personal communication, 1984) using data

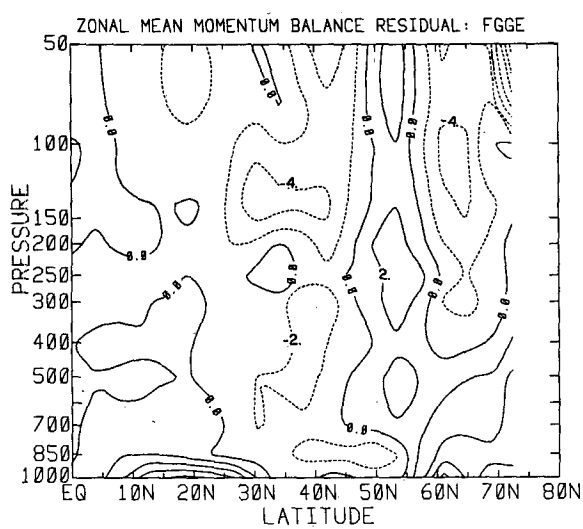

FIG. 10. Momentum balance residual for FGGE data. Contour interval of 2 m s^{-1} $(day)^{-1}$. Negative values indicate that negative acceleration (drag) is needed to complete the momentum balance.

from the 1982/83 winter. According to Palmer, the negative acceleration could be accounted for by the breaking of vertically propagating gravity waves near the tropopause. His calculations indicate that these breaking waves could result in an acceleration of a few meters per second per day, which is what is required to complete the momentum balance.

It is not known exactly how reliable this calculation is, as there are several potential sources of error. The zonally-averaged eddy fluxes are not known precisely, due to sparse sampling by radiosondes and the analysis techniques. Lau (1984) has compared such terms for GFDL and ECMWF analyses of the FGGE data and found considerable discrepancies. Another potential source of error is the strength of the mean meridional circulation. Sensitivity tests adjusting the strength of the circulation (not shown) did not tend to reduce the magnitude of the momentum residual, although a slightly weaker circulation produced a more uniformly negative residual. In addition to these data problems, a finite differencing of the momentum equation introduces some errors.

The FGGE data set is probably the best representation of a single winter that is available. The result presented here represents a best estimate of the actual residual. T. N. Palmer (personal communication, 1984) has obtained a similar result with an independent data set (1982/83 winter), which indicates that the result probably does not depend too much on the exact method of data analysis. It is also encouraging that there is a theoretical reason (breaking gravity waves) to expect a result similar to this. In any case, there must be some effect from sub-gridscale eddies, so that an exact balance cannot be expected.

5. Concluding remarks

Although Eliassen–Palm diagrams are very useful diagnostics in both the troposphere and the stratosphere, the EP flux divergence is not closely related to the mean wind acceleration. Thus the idea that $\nabla \cdot \mathbf{F}$ is the sole forcing of the mean flow by the eddies can be misleading. This result may partly reflect the fact that even the best data sets do not adequately represent all the terms in the zonal momentum equation. Calculations of the residual, the sum of all the terms in the zonal momentum equation, indicate that a coherent pattern with considerable negative (and in some places positive) acceleration is needed to complete the momentum balance. As suggested by T. N. Palmer (personal communication, 1984), this could be largely accounted for by the breaking of vertically propagating small-scale gravity waves near the tropopause. Failure to include this effect must certainly alter the momentum balance in general circulation models.

The present study does not prove that small scale waves are responsible for the residual, but should be regarded as further evidence that there is a significant problem in the momentum budget.

Acknowledgments. We wish to thank Dr. Eugenia Kalnay for providing the FGGE data. This work was supported by NASA Grant NAG5-233, and by the NSF's Atmospheric Research Section, NSF Grant ATM83-14111.

REFERENCES

Andrews, D. G., and M. E. McIntyre, 1976: Planetary waves in horizontal and vertical shear: The generalized Eliassen–Palm relation and the zonal mean acceleration. *J. Atmos. Sci.*, **37**, 2600–2616.

——, and ——, 1978: Generalized Eliassen–Palm and Charney–Drazin theorems for waves on axisymmetric mean flows in compressible atmospheres. *J. Atmos. Sci.*, **35**, 175–185.

Boyd, J. P., 1976: The noninteraction of waves with zonally-averaged flow on a spherical earth and the interrelationships of eddy fluxes of energy, heat and momentum. *J. Atmos. Sci.*, **33**, 2285–2291.

Charney, J. G., and P. G. Drazin, 1961: Propagation of planetary scale disturbances from the lower into the upper atmosphere. *J. Geophys. Res.*, **66**, 83–109.

Dunkerton, T., C.-P. F. Hsu and M. E. McIntyre, 1981: Some Eulerian and Lagrangian diagnostics for a model stratospheric warming. *J. Atmos. Sci.* **38**, 819–843.

Edmon, H. J., B. J. Hoskins and M. E. McIntyre, 1980: Eliassen–Palm cross-sections for the troposphere. *J. Atmos. Sci.*, **37**, 2600–2616.

Hartmann, D. L., and C. R. Mechoso and K. Yamazaki, 1984: Observations of wave-mean flow interaction in the Southern Hemisphere. *J. Atmos. Sci.*, **41**, 351–362.

Lau, N.-C., 1984: A comparison of circulation statistics based on FGGE III-B analyses produced by GFDL and ECMWF for the special observing periods. NOAA Data Rep. ERL GFDL-6, xx pp.

Oort, A. H., 1983: Global Atmospheric Circulation Statistics, 1958–1973. NOAA Prof. Pap. 14, U.S. Dept. of Commerce, Washington, DC., 180 pp.

——, and E. M. Rasmusson, 1971: Atmospheric Circulation Statistics. NOAA Prof. Pap. 5, U.S. Dept. of Commerce, Washington, DC., 323 pp.

Palmer, T. N., 1981: Diagnostic study of wavenumber-2 stratospheric sudden warming in a transformed Eulerian-mean formalism. *J. Atmos. Sci.*, **38**, 844–855.

——, 1982: Properties of the Eliassen–Palm flux for planetary scale motions. *J. Atmos. Sci.*, **39**, 992–997.

Quiroz, R. S., 1979: Tropospheric–stratospheric interaction in the major warming event of January–February 1979. *Geophys. Res. Lett.*, **6**, 645–648.

Strauss, D. M., 1983: Conservation laws of wave action and potential vorticity for Rossby waves in a stratified atmosphere. NASA Tech. Memo. 86058, GLAS, Goddard Space Flight Center, Greenbelt, MD 20771.